Structure and energetics of Ni and Au nanoclusters deposited on the (001), (110), and (111) surfaces of Au and Ni: A molecular dynamics study

De Nyago Tafen* and Laurent J. Lewis†

Département de Physique and Regroupement Québécois sur les Matériaux de Pointe, Université de Montréal, Case Postale 6128, Succursale Centre-Ville, Montréal, Québec, Canada H3C 3J7

(Received 19 October 2007; published 26 February 2008)

We present a comprehensive theoretical study—within the framework of the embedded-atom method—of the structural properties of Ni and Au nanoclusters deposited on the (001), (110), and (111) surfaces of Au and Ni, respectively, to characterize the evolution of the interfaces between nanoparticles and substrates. The Ni nanoclusters are found to exchange with the Au substrate atoms to form subsurface wetting layers. The exchanges occur either in a concerted fashion with the formation of a transient dimer, or in a two-step process consisting of complete insertion, then ejection of substrate atoms. Our results show a significant dependence of the shape of the embedded nanocluster on the surface, temperature, and contact angle. In contrast, Au nanoclusters do not burrow into Ni surfaces; embedded clusters resurface to either form an extra layer on the surface or alloy with the topmost substrate layer.

DOI: 10.1103/PhysRevB.77.075429 PACS number(s): 68.47.De, 61.46.Bc, 61.30.Hn, 68.08.Bc

I. INTRODUCTION

In the past few years, the study of materials (atoms, small clusters, nanoparticles, etc.) deposited on metal substrates has considerably developed, showing a large variety of structural behaviors.[1–7] A specific example is the site-exchange process that can result in the formation of surface alloys even for metals immiscible in bulk form. Here, single adatoms exchange with substrate atoms so as to minimize the energy of the system; this process has been found to be an effective diffusion (mass transport) mechanism.[8] The burrowing of clusters into the substrate—a "superexchange" mechanism whereby clusters as a whole bury under the surface—has also been reported: Co clusters, for example, are found to burrow into Au(111), Cu(100), and Ag(100) substrates.[2,3,9,10]

Experimental studies by Padovani *et al.* have shown that Co clusters burrow into Au(111) surface at a temperature of about 450 K.[3] This behavior, which can lead to surface smoothing, is driven by capillary forces that cause material to flow along the cluster-substrate interface.[2] Classical molecular dynamics simulations have shown that the burrowing mechanism depends on the configuration of the cluster after thermal deposition.[9] Deposited clusters with an epitaxial configuration burrow through vacancy migration along the cluster-substrate interface, while nonaligned clusters burrow through the disordered motion of atoms. It was suggested that burrowing should occur in all systems where the nanoparticles have a significantly higher surface energy than the substrate; if the nanoparticles have a smaller surface energy, they would simply wet the substrate.[2] For transition metal surfaces, these two mechanisms—burrowing and wetting—and the competition between them are still not well understood.

In the present paper, we investigate the deposition of Ni nanoclusters on Au surfaces as well as Au nanoclusters on Ni surfaces; the surfaces considered are (001), (110), and (111). Anticipating our results, we find that Ni nanoclusters burrow into Au substrates, whereas Au nanoclusters do not penetrate into the Ni surfaces. Ni and Au being almost immiscible in the bulk, this difference is somewhat surprising. The fact that Ni has a larger surface energy than Au would be expected to lead to the formation of a thin layer of substrate atoms around the nanocluster. Our aim is to understand what causes the difference between the two situations, and why one favors burrowing and the other surface wetting. In the burrowing process, the atomic exchanges provide an effective mechanism for cluster propagation into the substrate, which is absent in wetting. In the latter, the movement of atoms proceeds by jumps. Another question that arises is the most probable shape of the embedded cluster when burrowing takes place. Depending on the temperature, deposited nanoparticles can substitute for substrate atoms at the surface and form a so-called surface alloy. These atoms can also diffuse through the substrate and locate themselves underneath the surface layer, thus leading to subsurface wetting. To address these questions, we proceed in two steps: first, molecular statics (MS) calculations so as to obtain the relaxed configurations of the systems, then molecular dynamics (MD) simulations to investigate their evolution in time. We find a clear tendency for the embedded Ni atoms to form subsurface layers within the Au substrates. In addition, Au nanoclusters forced to be embedded within Ni substrates resurface to form an extra layer on the substrate or to alloy with the topmost substrate layer.

II. MODEL AND CALCULATIONS

The (atomic scale) calculations presented in this paper were performed using the program GROF, a multipurpose MD code developed largely by one of the authors (L.J.L.). The atom-atom interactions are described in terms of the embedded-atom method of Foiles *et al.*[11] using the parametrization proposed by Adams *et al.*[12] This model is semiempirical in the sense that it approaches the total energy problem from a local electron-density viewpoint, but using a functional form with parameters fitted to experiment (equilibrium lattice constant, sublimation energy, bulk modulus, elastic constants, etc.).

TABLE I. Details on the models used in the present calculations. N_{layer} is the number of layers forming the slab and $N_{at/layer}$ is the number of atoms per layer.

	Ni/Au		Au/Ni	
Surface	N_{layer}	$N_{at/layer}$	N_{layer}	$N_{at/layer}$
(001)	13	484	17	484
(110)	15	408	24	330
(111)	13	400	16	400

Atomic models for each of the three different types of surfaces were constructed in a slab geometry, viz. periodic boundary conditions along the x and y directions, parallel to the plane of the surface, and free boundaries in the z direction, normal to the surface; the bottom two layers were, however, fixed to mimic the presence of the (infinite) bulk. Other details—number of layers in the slabs and number of atoms per layer—are listed in Table I. The slabs were relaxed to their minimum energy configuration using MS before addition of the clusters; in all cases, this induced a contraction in the top interlayer spacing.

For both Au and Ni, clusters consisting of 240 atoms, and roughly spherical in shape, were first prepared and relaxed at 0 K using MS minimization. These were then placed close to the surface (Ni and Au, respectively), at a distance of 2.69 Å, corresponding to the average Au-Ni nearest-neighbor distance in the bulk. The evolution of the system from then on—followed using classical MD—is very slow and depends, in particular, on temperature. The observed behavior is quite similar to that for the coalescence of two clusters:[13] in a first stage, the contact surface is maximized; this then increases slowly until the adsorbate cluster starts sinking and/or spreading on the surface.

The results for the evolution of the systems will be analyzed in terms of the formation energy of a given configuration. Let δE be the "energy of inclusion" per cluster atom:

$$\delta E = \frac{\Delta E^{\mathrm{emb}} - \Delta E^{0}}{N_{\mathrm{cluster}}}, \tag{1}$$

where ΔE^{0} is the adsorption energy of the cluster on the surface, ΔE^{emb} is the formation (embedding) energy of the inclusion, and N_{cluster} is the size of the nanocluster. For the case of Au clusters manually embedded in Ni substrates, we may write

$$\Delta E^{\mathrm{emb}} = E^{\mathrm{emb}}_{\mathrm{Ni+Au}} - E^{\mathrm{mat}}_{\mathrm{Ni}} - E_{\mathrm{Au}}, \tag{2}$$

where

$$E^{\mathrm{mat}}_{\mathrm{Ni}} = E^{\mathrm{free\ surface}}_{\mathrm{Ni}} - N^{\mathrm{rem}}_{\mathrm{Ni}} E^{\mathrm{bulk}}_{\mathrm{Ni}}. \tag{3}$$

In the above, $E^{\mathrm{emb}}_{\mathrm{Ni+Au}}$ is the total energy of the slab *with* the inclusion, E_{Au} is the total energy of an isolated Au cluster, $E^{\mathrm{free\ surface}}_{\mathrm{Ni}}$ is the total energy of the clean Ni surface, $E^{\mathrm{bulk}}_{\mathrm{Ni}}$ is the energy per Ni atom in the bulk, and $N^{\mathrm{rem}}_{\mathrm{Ni}}$ is the number of Ni atoms removed from the slab by the inclusion.

Microcanonical-ensemble MD simulations covering up to several nanoseconds were performed at temperatures T =700 and 800 K; these temperatures were chosen in part to accelerate the dynamics. Some test calculations at temperatures lower than 700 K were also carried out; we found that burrowing does not take place at temperatures $\leqslant$300 K, whereas at temperatures above 300 K (but less than 600 K), very few atoms sink into the substrate after running more than 13 ns. This is consistent with the experiments of Zimmermann *et al.*,[2] which show that Co nanoparticles on clean Cu(100) and Ag(100) substrates do not burrow or even reorient.

TABLE II. Calculated exchange energy barriers (in eV) for Ni atoms on Au surfaces and Au atoms on Ni surfaces. The energy differences ΔE between initial and final states for the exchanges are also given.

Surface	Ni/Au		Au/Ni	
(001)	0.2088	0.20[a]	1.3363	
(110)	0.4614		0.4576	0.56[a]
(111)	0.5768		1.8274	1.70[b]
		ΔE (eV)		
(001)	−0.048		0.206	
(110)	−0.043		0.106	
(111)	−0.418		0.234	

[a]Reference 14.
[b]Reference 15.

III. RESULTS AND DISCUSSION

A. Exchange energies

The site-exchange process, whereby an adatom changes place with one (or more) surface atom(s), is a peculiar diffusion mode for transition metal surfaces.[16–20] In heterogeneous deposition, the surface morphology and crystal growth can be strongly influenced by the occurrence of such processes. Exchanges promote surface mobility provided that the energetics and kinetics favor this mechanism over hopping. They also drive the incorporation of foreign atoms into the substrate, leading to surface alloying. In order to better understand the kinetics of our surfaces, including possible alloying effects, and before proceeding to the more complicated nanocluster-substrate case, we calculated the exchange energies for single adatoms using the nudged elastic band method.[21] The results are listed in Table II, where we also give other values from the literature. The barriers for the exchange of a Ni adatom with a Au surface atom are generally lower than those for the opposite situation. In our calculations, the energy *difference* ΔE between initial and final states for the exchange of a Ni atom with a Au surface atom is negative (cf. Table II), indicating that the process is energetically favorable. In the case of a Au atom exchanging with a Ni surface atom, now, the barriers are much larger, except for Ni(110) where it is comparable; also, unlike the previous case, the energy difference is positive. To our knowledge, no experimental data are available for the exchange barriers.

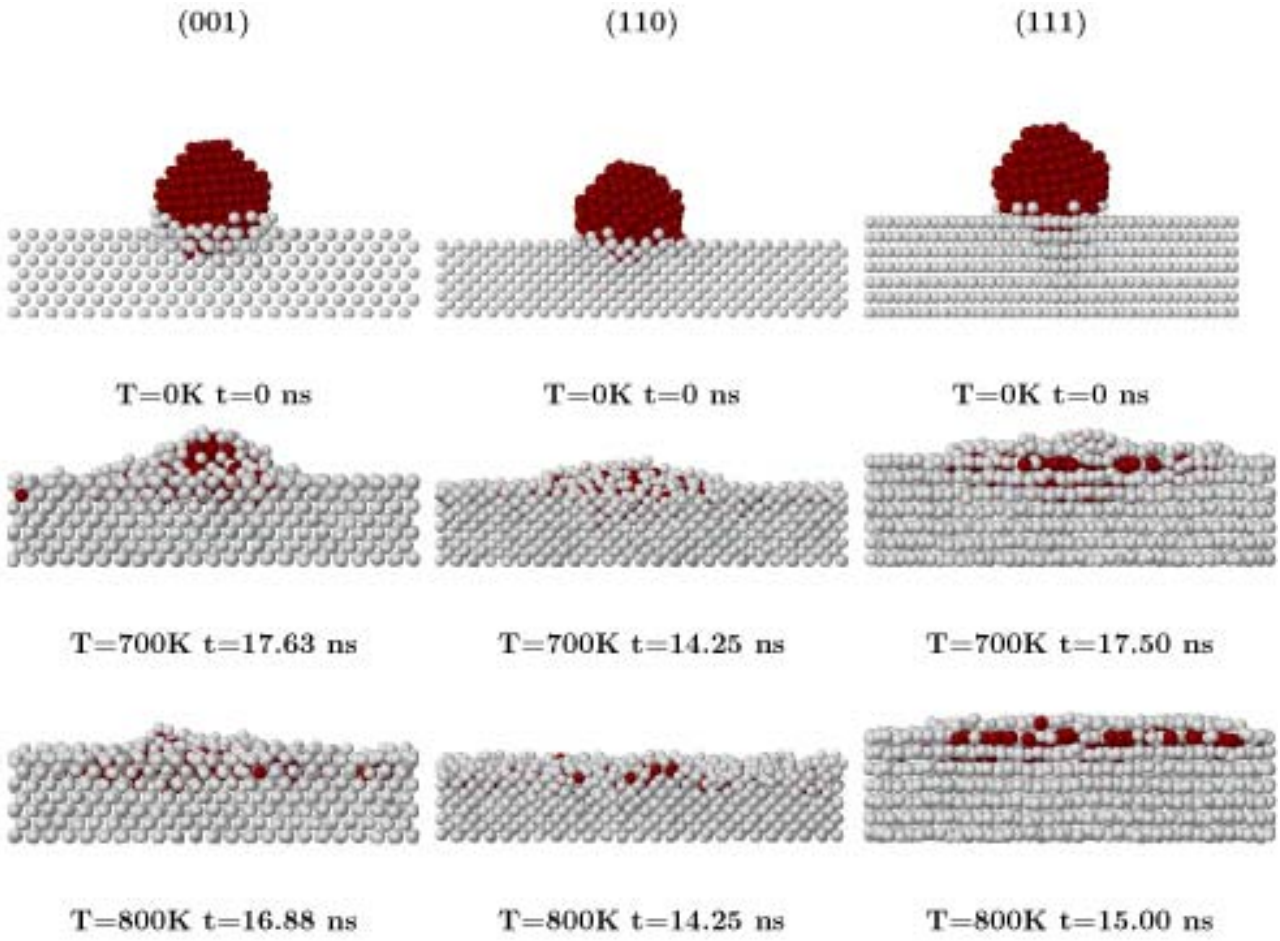

FIG. 1. (Color online) Burrowing of a 240-atom Ni nanocluster (red) into (001), (110), and (111) Au surfaces (gray). The top panels show the initial, MS-relaxed configurations. The middle panels show the state of the clusters at 700 K after 17.63, 14.25, and 17.50 ns, respectively, when the cluster has just burrowed. The bottom panels present the corresponding data at 800 K after 16.88, 14.25, and 15.00 ns, respectively. (The times are somewhat arbitrary and are such that the systems no longer evolve.) For clarity, the six bottommost layers are not represented.

Our results are in good agreement with the first-principles results of Tersmentzidis *et al.*[15] for Au/Ni(111) and the semiempirical results of Deutsch *et al.*[14] for Ni/Au(001) and Au/Ni(110), and also with the energy gain during the exchange process obtained *ab initio* by Stepanyuk and Hergert.[22]

The mechanisms underlying the exchange process differ from one surface to another. For Ni/Au(001), Ni/Au(110), Au/Ni(001), and Au/Ni(110), exchanges occur in a concerted fashion with the formation of a dimer at the transition state; here, the adatom and the substrate atom move in unison during the transition. For Ni/Au(111), the exchange proceeds in two steps: complete insertion of the adsorbate Ni atom, then ejection of a Au surface atom; this two-step process accounts for the high tensile surface stress of Au(111) caused by the large surface mismatch.[20] The two-step process is also seen in the case of Au/Ni(111). The difference here is that the ejection of a Ni atom occurs before the insertion of a Au atom; in this case, Ni atom needs extra energy in order to move from its equilibrium position and overcome the barrier.

B. Ni clusters on Au surfaces

We examine now the interaction of clusters with surfaces, starting with the case of Ni_{240}/Au. First, we computed the lowest-energy structures by performing MS (steepest descent and conjugate gradient) relaxation, from which we can obtain the adsorption energies E_{ads} (per cluster atom); the values for the three surfaces are given in Table III, with the lowest value corresponding to the (110) surface. Next, MD simulations were performed in order to investigate the kinetics of relaxation at finite temperature; this is illustrated in

TABLE III. Calculated adsorption energies E_{ads} and embedded energies ΔE^{emb} for Ni nanoclusters on Au surfaces; all energies are in eV per Ni atom.

Au Surface	E_{ads}	ΔE^{emb}
(001)	−0.152	−0.496
(110)	−0.162	−0.472
(111)	−0.135	−0.466

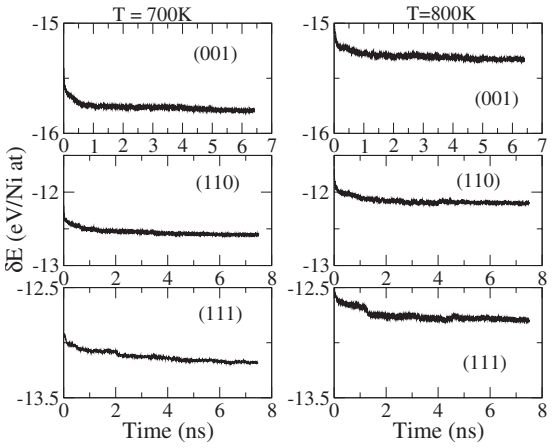

FIG. 2. Inclusion energies for Ni_{240} on the (001), (110), and (111) surfaces of Au as a function of time; $t=0$ corresponds to the MS-relaxed configuration.

Fig. 1. We find that the nanoclusters do not remain on the surfaces but, rather, burrow into the substrates, simultaneously expelling gold atoms that, in turn, contribute to embed the nanoclusters. Concomitantly, the inclusion energies drop as a function of time, as displayed in Fig. 2, eventually reaching a stable value (which depends on temperature). The inclusion energy is found to be lowest for the (001) surface.

From Fig. 1, it is seen that the nanoclusters adopt random distributions when embedded into the substrates, in agreement with recent *ab initio* results.[22] This characteristic feature suggests that the nearest-neighbor attractive interaction between Ni atoms in the gold surfaces are effectively suppressed, leading to a solid solution with a strong tendency to disordering.

Figure 1 reveals a pronounced difference in the surface topographies between 700 and 800 K: the majority of atoms have sunk into the substrate, except on the (001) surface at 700 K, and the surfaces are much smoother at 800 K, driven by the higher thermal energy. The Ni nanocluster becomes completely coated with Au atoms, the former, thus, now forming a "subsurface wetting" layer; we will return to this point below.

The adsorption energies E_{ads} are compared in Table III with the energies required to embed the clusters in the substrates, ΔE^{emb}. The embedding energies are two or three times larger than the adsorption energies, the lowest value corresponding to the (001) surface. This large difference indicates that the nanoclusters preferentially sink into the substrate rather than remain on the surface. This is in complete agreement with the calculations of Ruban *et al.*,[23] who found Ni atoms to "antisegregate" on Au substrates.

In order to better understand the burrowing process and the change in shape of the nanoclusters, we computed the average density profiles $\rho(z)$ before and after MD relaxation, with $\rho(z)dz$ the number of atoms in a slice of thickness dz at z; peaks in $\rho(z)$ correspond to layers and their integral gives the total number of atoms in the layers. These are displayed in Figs. 3–5. After relaxation, the nanoclusters extend over two layers or more below the surface, with a strong dependence on both surface and temperature. For the (001) surface, the nanocluster lies on two subsurface layers at 800 K, compared to four at 700 K, as it does not penetrate the substrate completely. For the (110) surface, the nanocluster occupies five subsurface layers at 800 K, and is covered with a thick coat of substrate Au atoms. The (111) surface, finally, behaves differently: the Ni atoms form two subsurface layers at 800 K, and four layers at 700 K; while this is similar to the results for the (001) surface, we observe a clear tendency here for atoms to form "true" subsurface layers, i.e., at the exact positions of the Au substrate layers.

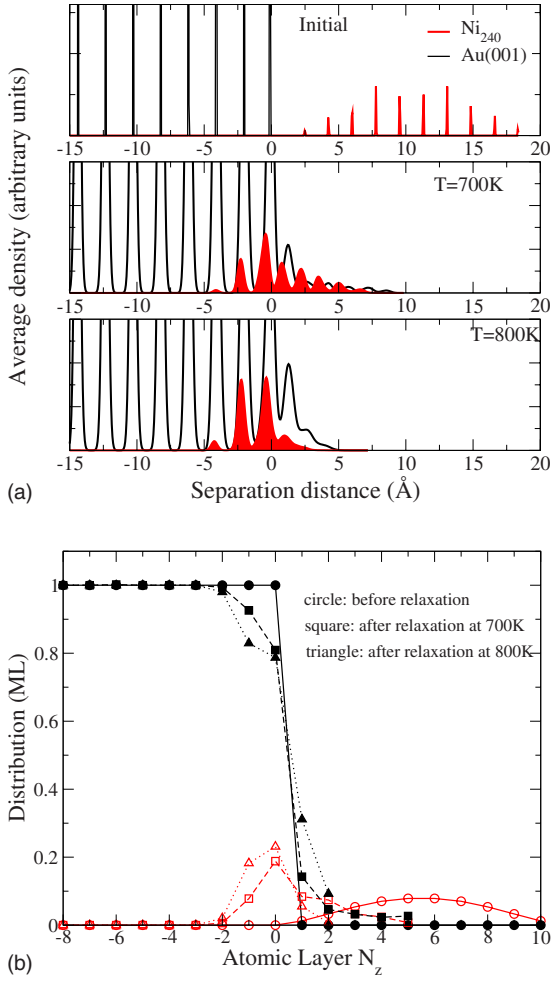

FIG. 3. (Color online) Top: Average density profiles for Ni_{240} on the Au(001) surface in the initial state, and at 700 and 800 K, as indicated. The three bottommost layers are not represented. Bottom: Integral of the density profiles showing the distribution of nickel (red) and gold (black) atoms before and after relaxation; this is measured in ML, 1 ML corresponding to the number of gold atoms per substrate layer (see Table I).

The distribution of Ni and Au atoms following the relaxation process can be obtained by integrating the density profiles discussed above. The distribution of Au atoms, initially a step function, becomes nearly continuous for all three surfaces, thus confirming the formation of subsurface layers. The distribution of Ni and Au differs from one surface to another and depends on temperature. For the three surfaces, we find that as the Ni cluster sinks into the substrate, Au atoms are expelled; the ousted Au atoms form extra layers at

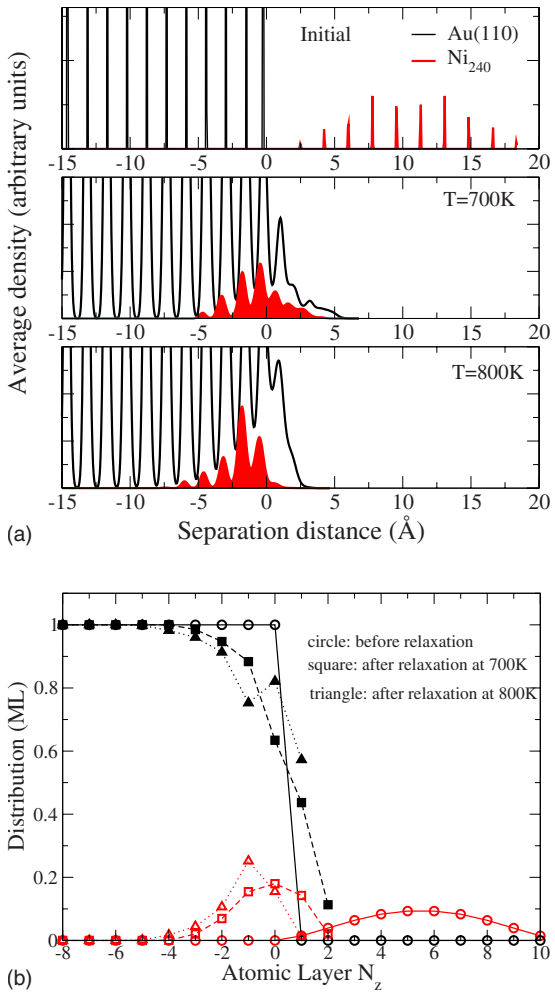

FIG. 4. (Color online) Same as Fig. 3, but for Ni_{240}/Au(110).

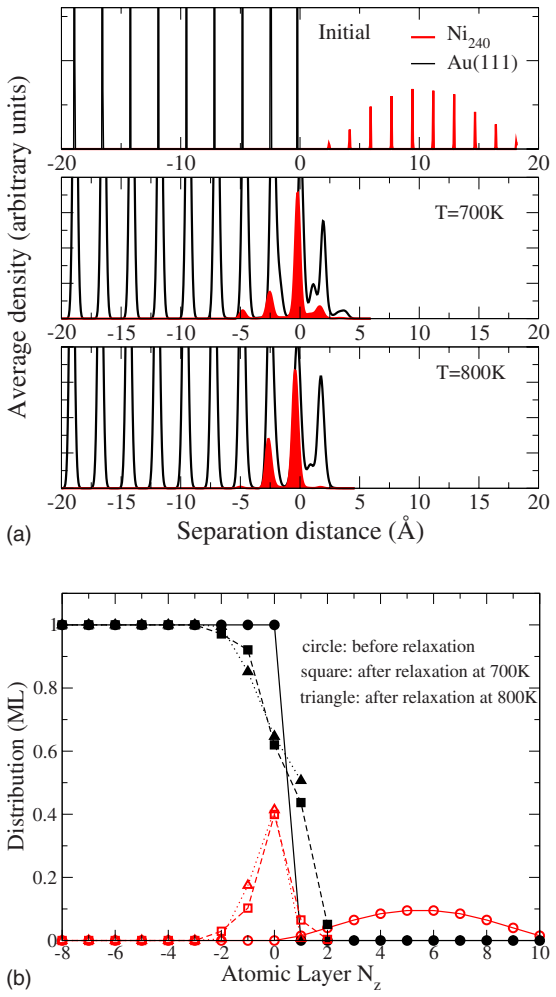

FIG. 5. (Color online) Same as Fig. 3, but for Ni_{240}/Au(111).

the surface. These layers originate mostly from the initial surface [labeled N_z=0; ~0.213 ML (monolayer)] and the first two layers just below the original surface of the substrate. Furthermore, it may be seen in Figs. 3–5 that a large concentration of Ni atoms is located underneath a gold layer.

We have examined the impact on burrowing of varying the contact angle (α) between the substrate and the absorbate; this is related to the diffusion through the cluster-substrate interface. The contact angle was varied by changing the orientation of the nanocluster while keeping it as closely spherical as possible. We found the embedding energies to vary little with α. In contrast, the shape of the embedded nanocluster varies significantly with α. This can be seen in Fig. 6, where we plot the concentration of cluster atoms (Ni) within specific substrate layers as a function of α. Though statistics are limited, the general trend is that the concentrations vary roughly linearly with α, i.e., the depth reached by the cluster depends on how it was initially positioned on the surface. This suggests that some sort of cooperative motion of atoms is involved when, for example, the initial contact is epitaxial.

C. Au clusters on Ni surfaces

In sharp contrast to the preceding case, Au clusters wet Ni surfaces, i.e., spread to form a thin film on top of the substrate as illustrated in Fig. 7. For the (001) and (111) sur-

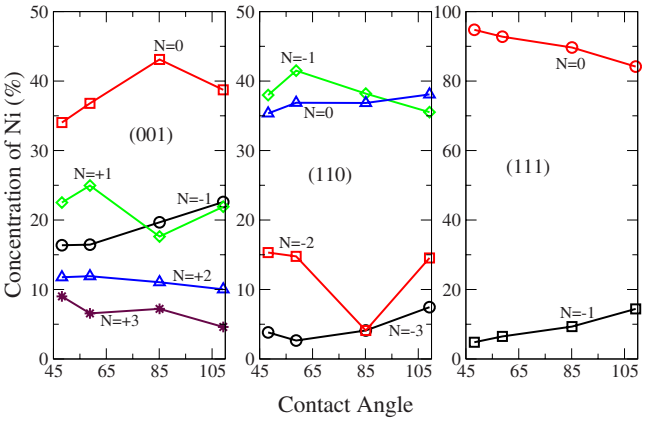

FIG. 6. (Color online) Concentration of cluster atoms (Ni) within specific substrate layers as a function of contact angle α.

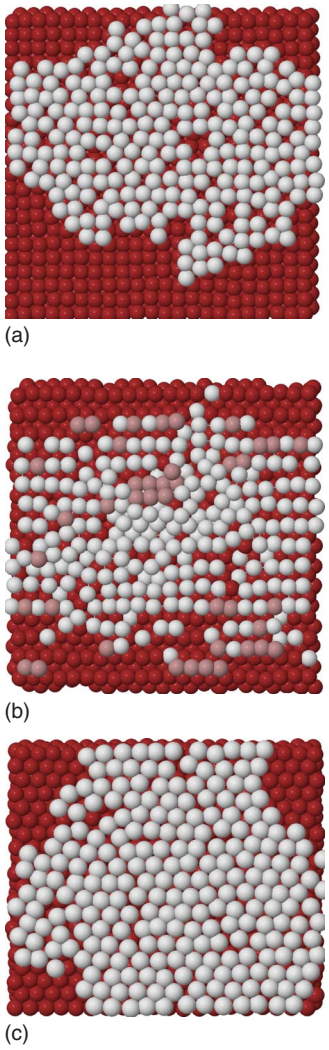

FIG. 7. (Color online) Wetting structures for Au_{240} on (a) Ni (001), (b) (110), and (c) (111). Au atoms are gray, and Ni atoms are red; for the (110) surface, the Ni atoms expelled from the surface are pink.

faces, none of the Au atoms have sunk into the Ni substrate even at 800 K. In the (110) case, however, a significant proportion of Au atoms exchange with Ni atoms in the first layer, forming a surface Au-Ni alloy; the squeezed-out Ni atoms agglomerate and form dimers and Ni chains on the surface (colored in pink in Fig. 7). This is consistent with our results for the exchange energies presented in Table II: the barrier for Au/Ni exchange is much lower on the Ni (110) surface than on either (001) or (111). Similar results were obtained by Nielsen *et al.*[24] using scanning tunneling microscopy, and by Fan and Gong[25] using Monte Carlo simulations.

Thus, burrowing does not take place for Au nanoclusters on Ni surfaces. We calculated the wetting energy—the energy required for the spherical nanocluster to wet the surface—for the three surfaces; the results are given in Table IV. This is lowest for the (110) surface, presumably because of surface alloying.

In order to understand the adsorption (vs burrowing) behavior, we have performed two other types of calculations.

TABLE IV. Calculated adsorption energies E_{ads}, inclusion energies δE, and wetting energies δE^w for Au nanoclusters on Ni surfaces; energies are in eV per Au atom.

Ni Surface	E_{ads}	δE	δE^w
(001)	−0.10504	+0.21949	−0.70509
(110)	−0.23954	+0.35465	−0.78283
(111)	−0.09785	+0.26488	−0.66458

First, we have calculated the nanocluster embedding energies for the three different surfaces using MS calculations. The nanoclusters were, thus, embedded manually in the substrates, then relaxed to their minimum energy configurations. Embedding leads to a very significant increase of the energy of the interface; Table IV summarizes the calculated [using Eqs. (1)–(3)] energy differences for initially spherical nanoclusters. After relaxation, the shapes of the inclusions change noticeably, but they remain compact. In all three cases, the embedding energy is positive, corresponding to an endothermic process, and is, thus, not favored.

Second, we have performed MD simulations of Au_{240} embedded in a Ni substrate having either one or two free surfaces in order to study the dynamics of "unburrowing." In Fig. 8, we present the results for the system with a single free surface. The gold atoms diffuse toward the surface and emerge to either form an extra layer on the substrate or alloy with the topmost substrate layer. For the geometry with two free surfaces, a Ni layer forms on both surfaces. These results are consistent with the surface segregation energy calculations of Ruban *et al.*[23]

Finally, we examined the stress distribution in the nanocluster and in the substrate for each configuration. The atomic level stresses are calculated using[26]

$$\sigma_{\alpha\beta}(i) = -\frac{1}{\Omega_0}\left[\frac{p_i^\alpha p_i^\beta}{m_i} + \frac{1}{4}\sum_j (r_{ij}^\beta f_{ij}^\alpha + r_{ij}^\alpha f_{ij}^\beta)\right], \qquad (4)$$

where $(\alpha,\beta) \equiv (x,y,z)$, m_i and $\vec{p}_i$ are the mass and momentum of atom i, $\vec{r}_{ij}$ is the distance from atom i to j, $\vec{f}_{ij}$ is the force on atom i due to j, and Ω_0 is the average atomic volume. Figure 9 shows the atomically resolved stress distribution, $P_\sigma = \mathrm{Tr}(\sigma_{\alpha\beta})$, along z at $x=0$, $y=0$. The sinking nanocluster leads to an inhomogeneous stress distribution in the substrate. In the case of Ni_{240} on Au, the stress P_σ changes abruptly from tensile (free surface) to compressive over the bottom atomic layers of the substrate, and from compressive ($N_z < -10$) to tensile, reaching a maximum value and nearly going to zero at the topmost atomic layer. In the tensile region, $-10 \leqslant N_z \leqslant 5$, there is a very high concentration of Ni atoms.

For Au_{240} on Ni, the behavior of the corresponding stresses is completely different, especially for Ni(110) where the stress remains tensile compared to the free surface, which is highly tensile. For the latter, the presence of stress plays a crucial role in the surface diffusion by lowering the energy barrier for exchanges. The surface diffusion proceeds by atomic exchanges between Au atoms and Ni substrate atoms

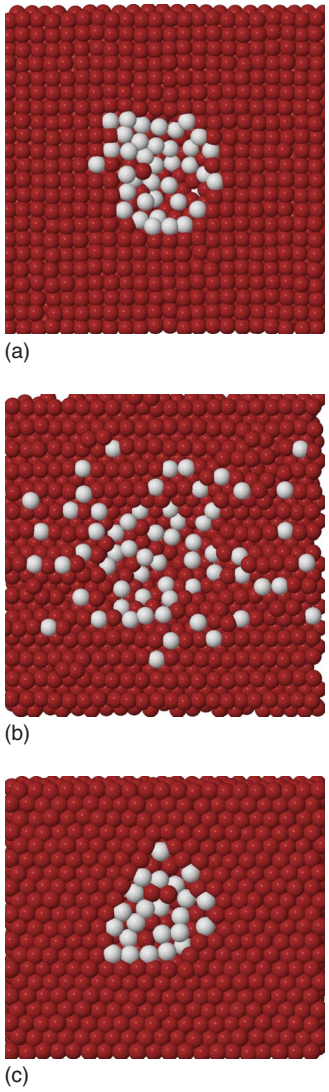

FIG. 8. (Color online) Structure of an embedded Au_{240} cluster in (a) (001), (b) (110), and (c) (111) Ni surfaces obtained by MD simulations for the system with a single free surface. Au atoms are gray, and Ni atoms are red.

with the formation of a Au-Ni surface alloy. This analysis is consistent with the results of Yu and Scheffler for fcc(100) transition metal surfaces.[27] On the two other surfaces, the stress is compressive in the substrate and becomes tensile at the wetting layer. Since the stress and the strain are intimately related, it is reasonable to expect that burrowing will cost less energy for a surface under significant tensile strain than for a compressed surface. As the substrate suffers tensile strain, adatoms are better able to relax into the substrate surface, increasing their local electron density, thereby increasing their adsorption energy.

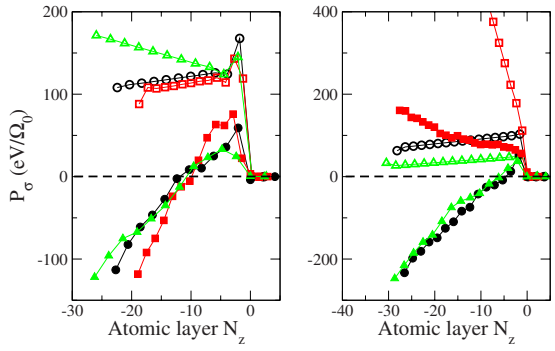

FIG. 9. (Color online) Stress distribution along z for Ni clusters burrowed in Au surfaces (left) and Au cluster wetting Ni surfaces (right). The open symbols represent stress in the free surfaces. Left panel [right panel]: circle, Au(001) [Ni(001)]; square, Au(110) [Ni(110)]; and triangle, Au(111) [Ni(111)]. The filled symbols represent the stress distribution for Ni_{240}/Au (left panel) and Au_{240}/Ni (right panel). N_z=0 denotes the initial uppermost substrate atomic plane.

IV. CONCLUSION

Using semiempirical calculations, we have investigated the structural properties of Ni and Au nanoclusters deposited on the (001), (110), and (111) surfaces of Au and Ni, respectively, in order to characterize the evolution of the interfaces between nanoparticles and substrates. Ni nanoclusters are found to exchange with the Au substrates to form subsurface wetting layers. The exchange occurs either in a concerted fashion with the formation of a transient dimer or in a two-step process (complete insertion and then ejection). Our results show that the shape of the embedded nanocluster is surface and temperature dependent. It is also demonstrated that the contact angle is an important factor in defining the shape of the embedded nanocluster. In this respect, the concentration of the embedded atoms on a subsurface layer varies linearly with the contact angle. Our results also show that Au nanoclusters embedded in Ni substrates at 700 and 800 K resurface to either form an extra layer on the surface or alloy with the topmost substrate layer [case of (110)].

ACKNOWLEDGMENTS

D.N.T. thanks LingTi Kong for help and useful discussions. This work has been supported by grants from the Natural Sciences and Engineering Research Council of Canada (NSERC) and the *Fonds Québécois de la Recherche sur la Nature et les Technologies* (FQRNT). We are grateful to the *Réseau Québécois de Calcul de Haute Performance* (RQCHP) for generous allocations of computer resources.

*Present address: Department of Physics, West Virginia University, Morgantown, WV 26506-6315, USA; denyago.tafen@mail.wvu.edu

†Author to whom correspondence should be addressed; laurent.lewis@umontreal.ca

[1] B. Nacer, C. Massobrio, and C. Félix, Phys. Rev. B **56**, 10590 (1997).

[2] C. G. Zimmermann, M. Yeadon, K. Nordlund, J. M. Gibson, R. S. Averback, U. Herr, and K. Samwer, Phys. Rev. Lett. **83**, 1163 (1999).

[3] S. Padovani, F. Scheurer, and J. P. Bucher, Europhys. Lett. **45**, 327 (1999).

[4] C. G. Zimmermann, K. Nordlund, M. Yeadon, J. M. Gibson, R. S. Averback, U. Herr, and K. Samwer, Phys. Rev. B **64**, 085419 (2001).

[5] M. Yeadon, M. Ghaly, J. C. Yang, R. S. Averback, and J. M. Gibson, Appl. Phys. Lett. **73**, 3208 (1998).

[6] V. S. Stepanyuk, D. V. Tsivline, D. I. Bazhanov, W. Hergert, and A. A. Katsnelson, Phys. Rev. B **63**, 235406 (2001).

[7] T. Deutsch and F. Lançon, J. Phys.: Condens. Matter **15**, 1813 (2003).

[8] J. Fassbender, R. Allenspach, and U. Durig, Surf. Sci. **383**, L742 (1997).

[9] J. Frantz and K. Nordlund, Phys. Rev. B **67**, 075415 (2003).

[10] N. A. Levanov, V. S. Stepanyuk, W. Hergert, D. I. Bazhanov, P. H. Dederichs, A. A. Katsnelson, and C. Massobrio, Phys. Rev. B **61**, 2230 (2000).

[11] S. M. Foiles, M. I. Baskes, and M. S. Daw, Phys. Rev. B **33**, 7983 (1986).

[12] J. B. Adams, S. M. Foiles, and W. G. Wolfer, J. Mater. Res. **4**, 102 (1989).

[13] L. J. Lewis, P. Jensen, N. Combe, and J.-L. Barrat, Phys. Rev. B **61**, 16084 (2000).

[14] T. Deutsch, Ph.D. thesis, Institut National Polytechnique de Grenoble, 1995.

[15] K. Termentzidis, J. Hafner, and F. Mittendorfer, J. Phys.: Condens. Matter **18**, 10825 (2006).

[16] J. D. Wrigley and G. Ehrlich, Phys. Rev. Lett. **44**, 661 (1980).

[17] G. L. Kellogg and P. J. Feibelman, Phys. Rev. Lett. **64**, 3143 (1990).

[18] C. L. Chen and T. T. Tsong, Phys. Rev. Lett. **64**, 3147 (1990).

[19] P. J. Feibelman, Phys. Rev. Lett. **65**, 729 (1990).

[20] H. Bulou and C. Massobrio, Phys. Rev. B **72**, 205427 (2005).

[21] H. Jónsson, G. Mills, and K. W. Jacobsen, in *Classical and Quantum Dynamics in Condensed Phase Simulations*, edited by B. J. Berne, G. Ciccotti and D. F. Coker (World Scientific, Singapore, 1998), p. 385.

[22] V. S. Stepanyuk and W. Hergert, Phys. Rev. B **62**, 7542 (2000).

[23] A. V. Ruban, H. L. Skriver, and J. K. Nørskov, Phys. Rev. B **59**, 15990 (1999).

[24] L. P. Nielsen, F. Besenbacher, I. Stensgaard, E. Lægsgaard, C. Engdahl, P. Stoltze, K. W. Jacobsen, and J. K. Nørskov, Phys. Rev. Lett. **71**, 754 (1993).

[25] W. Fan and X. G. Gong, Surf. Sci. **562**, 219 (2004).

[26] W. Yu and A. Madhukar, Phys. Rev. Lett. **79**, 905 (1997).

[27] B. D. Yu and M. Scheffler, Phys. Rev. B **56**, R15569 (1997).